IOSR Journal of Mathematics (IOSR-JM)
e-ISSN: 2278-5728, p-ISSN: 2319-765X. Volume 18, Issue 2 Ser. II (Mar. – Apr. 2022), PP 26-39
www.iosrjournals.org

Buoyancy Effect on MHD Nanofluid flow over a Porous Medium In the presence of Dufour and Ohmic Heating.

A. M. Okedoye[*1], J. S. Damisa[2], *B. B. Malemi*[3] and *Kelvin O. Ogboru*[4]
Department of Mathematics, Federal University of Petroleum Resources, Effurun, Nigeria.
*[*1]okedoye.akindele@fupre.edu.ng, [2]xdamisajohn226@gmail,com, [3]beautykingsley1@gmail.com*

Abstract:
The flow of nanofluid flow through a porous medium has attracted several authors in the field of science, engineering and several industries over the decades. The viscous force in Newtonian and non-Newtonian fluids causes friction in the motion of several fluids. However, Buoyancy effect on MHD nanofluid flow and the characteristics of the thermophysical properties of copper (Cu) -nanofluid over a porous medium in the presence of Dufour and Ohmic heating is considered in this study. The transformed governing equation is solved numerically using midpoint methods known as midrich method with Richardson extrapolation enhancement or deferred correction enhancement *The effect of increasing the value of the controlling parameters on the temperature distribution, local heat transfer rate, concentration of the fluid, local skin friction and the velocity of the fluid flow are illustrated graphically and discussed. It is observed that the presence of nanoparticle volume fraction, thermal radiation and porous media parameter in the flow field, reduces the rate of thermal boundary layer thickness of nanofluids and when there is increase in the Buoyancy coefficient factor and the Buoyancy coefficient ratio the skin friction increases, while the rate of heat and mass transfer at the* wall decreases.

Keywords: *Buoyancy effect, MHD, Nanofluid, Porous Medium, Dufour, Ohmic heating, thermal radiation. Thermo-physical properties, Richardson extrapolation.*
MSC 2020: *76A05, 76D05, 76W05.*

Date of Submission: 12-03-2022 Date of Acceptance: 28-03-2022

I. Introduction

Factors such as density and volume of fluid come into play when buoyancy is considered. Buoyancy reduces the weight of object due to the fact that buoyancy force is proportional to density which generally makes it easier to be lifted. Boat sailing, life vest floating on water, helium balloon rising in the air, iceberg floating on water and ship floating on ocean are possible as a result of the buoyancy force. Different authors have carried out various studies on the effect of buoyancy. Effect of buoyancy and thermal MHD flow over a stretching porous sheet using homotopy analysis method that when there is an increase in the buoyancy parameter, the fluid velocity increases and the thermal boundary layer decreases[1]. The effect of buoyancy force in MHD flow and heat transfer with effects of buoyancy, viscous and joules dissipation over a nonlinear vertical stretching porous sheet with partial slip is found to be more pronounce for a fluid with a small magnitude of prandtl number[2]. The velocity over the vertical increases with the increase of regular buoyancy parameters and thermal radiation but decreases with the increase in activation energy on MHD buoyancy induced nanofluid flow past a vertical surface[3].

The concept of MHD was initiated by Hannes Alfven which received recognition in the year 1970. Magnetic induction is the production of an electromotive force or voltage across an electrical conductor due to its dynamic interaction with a magnetic field[4]. Magnetic field induced current possesses significant effects which produces forces on fluid in the Navier-Stokes model of fluid dynamics and Maxwell's equations of electromagnetism[5]. MHD in relation to nanofluid possesses a high capability in enhancing thermal conductivity and heat transfer which has wide range of applications in sciences and engineering such as aerospace industry, chemical and petrochemical engineering, heat exchanger, nuclear reactor, combustion systems. In nanoparticles concentration and nanoparticles size on nanofluids viscosity with a wide range of temperatures the temperature reduces the viscosity mainly nanoparticles with high concentration[6,7]. Putting this into consideration, the dependence of nanofluid properties on temperature, volume fraction of nanoparticles, must be taken into account in order to predict the correct role of nanoparticles on heat transfer enhancement. This brought the idea of discussing the effects of viscosity and thermal conductivity of Al_2O_3–water nanofluid[8]. More recently, the

thermal conductivity relative to nanofluid for different copper oxide nanofluid volume fractions was analyzed[9]. An increase in the magnetohydrodynamic parameter enhances the fluid surface penetration in the vicinity of the wall, the increase in the radiation parameter leads to the increase in the temperature gradient and in turn enhances the velocity of the fluid in Magnetohydrodynamics (MHD) on heat transfer of nanofluid flow over a plate[10]. Musa *et al.* (2019) investigated the. The increase in the variable thermal conductivity parameter in unsteady MHD flow of nanofluid with variable properties over a stretching sheet in the presence of thermal radiation and chemical reaction results in the increase of the temperature of the nanofluid[11].There is an increase of thermal conductivity of Heat and Mass Transfer through a Porous Media of MHD Flow of Nanofluids with Thermal Radiation, Viscous Dissipation and Chemical Reaction Effects[12]. Bioconvection in MHD nanofluid flow with nonlinear thermal radiation and quartic autocatalysis chemical reaction past an upper surface of a paraboloid of revolution was studied[13]. The heat and mass transfer analysis for the MHD flow of nanofluid with radiation absorption was examined[14]

In flow mechanism, there is a relationship between the flow rate and energy through a porous medium. The velocity of fluid decreases with the increase in the porous media parameter while temperature increases with the increase in the porous media parameter[15]. Ohmic heating (OH) is the process whereby an electric current is passed through material with the primary purpose of heating them[16]. Ohmic heating does not require the transfer of heat through solid-liquid interface or inside solid particles once the energy is dissipated directly into the system, a large number of actual and potential application exist for ohmic heating (OH) which includes; evaporation, dehydration, fermentation, extraction, sterilization, pasteurization, heating of food, military field heating and so on. Analysis of hydromagnetic free convection turbulent fluid flow over an infinite vertical plate modeled using conservation equations of energy and momentum shows that the primary velocity increases with decreasing magnetic parameter (M), increases with increase in Hall parameter and also increases with increase in Grashoff number, while, the secondary velocity increases with decreasing magnetic[17]. The theoretical analysis that investigates the unsteady convective flow of nanofluid using Blasius Rayleigh-Stokes variable with slip effect was examined mathematically to determine the effect of moving slot parameter, thermal Grashof number and mass Grashof number on the flow[18]. While the application of unsteady mixed convective MHD flow of a viscous incompressible electrically conducting fluid past an accelerated infinite vertical porous flat plate with suction in presence of radiation in geophysical, astrophysical and cosmical shows that greater suction leads to a faster reduction in the velocity of the flow field, magnetic parameter retards the velocity of the flow field at all points also suction parameter is to enhance the skin friction, Nusselt number and Sherwood number at the wall[19].

Recently, the fluid limiting surface of heat and mass transfer in unsteady natural convection MHD boundary layer flow past a moving plate with binary chemical reaction assumed to move impulsively, with a constant velocity, either in the direction of the flow or in the opposite direction, in the presence of a transverse magnetic field. Both frequency-dependent effects and "long-time" effects that would require non-practically long channels to be observed in steady flow[20]. We also explored mathematically the important aspects of reactive fluid flow, especially the residence time flow behaviour, scale-up and scale-down procedures heat and mass transfer of unsteady MHD natural convective flow past a motioning plate with binary chemical reaction was observed that temperature is enhanced as the fluid angular velocity rises which leads to maximum temperature in the body of the liquid. It is discovered that mean velocity decrease with a rise in the species reaction and reaction order[21].The computational results for momentum and heat distribution of the flow of nonlinear magnetohydrodynamic (MHD), laminar, viscous, incompressible boundary layer fluid with thermal radiative heat transfer and variable properties past a stretching surface was observed that the parameters which enhanced the heat source terms decreased the fluid viscosity and caused increase in the flow rate[22].An unsteady flow of heat and species transport through a porous medium in an infinite movable vertical permeable flat surface with hydromagnetic chemical reactive fluid flow is stimulated by the thermal and solutant convection, and propelled by the movement of the surface revealed that the species boundary layer increases with a generative chemical reaction and decreases with a destructive chemical reaction[23]. The analysis on the transient double diffusion of a binary mixture in a porous moving flat device without viscoelasticity of the reactive fluid and material deformation, the considered fluid satisfied Newtonian properties with continuous molecular collision under convection and magnetic field influence, the reaction is motivated by chemical heat generation and Arrhenius kinetics, reveal that a monotonically increase in the thermal diffusion is strongly impacted by an increasing value of heat generation and radiation throughout the flow regime.[24]

However, in some condition where the concentration of the particles is high, that same low conductivity particle may transfer heat faster than the surrounding fluid[25]. With the phenomenon described above, it shows that there is an increase in particle concentration of the fluid. This would lead to higher percentage of current flowing through the particles of the solid than the percentage of current flowing through the particles of the fluid when electric current is passed through the system. It is in view of the above literatures, we intend to bridge the gap by providing. Our motivation is drawn from the fact that the effects Buoyancy on

MHD nanofluid flow over a porous medium in the presence of Dufour and ohmic heating have not been properly dealt with. In view of the above, we intend to bridge the gap by providing our investigation on the subject matter.

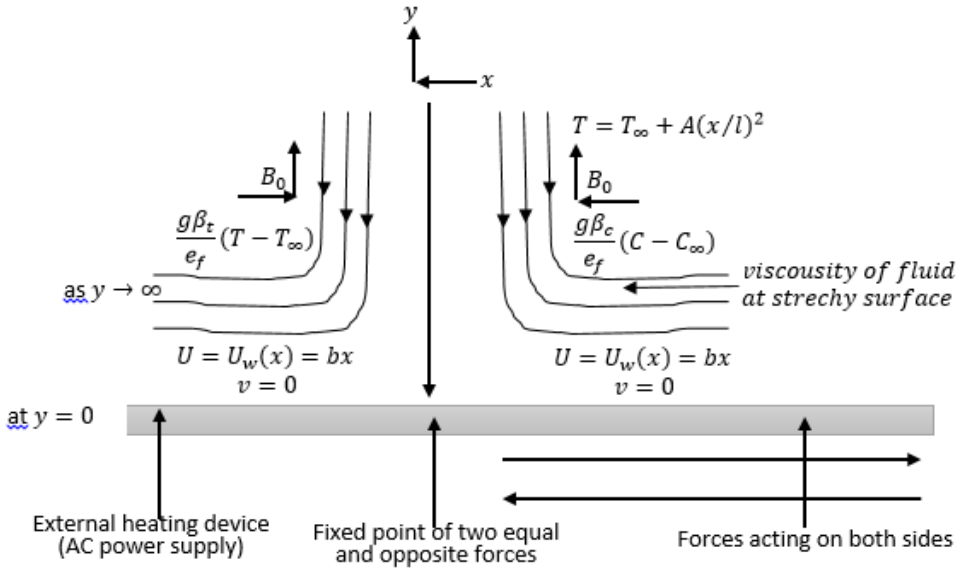

Figure 1: Flow configuration and coordinate system

II Mathematical Analysis

Consider a two dimensional steady laminar boundary layer flow of an incompressible nanofluid over a stretching sheet. The *x-axis* is taken along the direction of the continuous stretching surface and the *y-axis* is measured normal to the surface of the sheet. A uniform transverse magnetic field of strength B_0 is applied in the direction of *y-axis*. The flow is continuous due to stretching of the sheet, it is assumed that the induced magnetic field and the electric field due to polarization of charges are negligible in comparison to the applied magnetic field. The flow configuration and coordinate system is shown in Figure 1.

The fluid is water (H_2O) based nanofluid containing copper (Cu) nanoparticles. It is assumed that the based fluid and the nanoparticles are in thermal equilibrium and no slip occurs between them. It is also assumed that the surface has temperature T_w and concentration C_w, the fluid has ambient temperature T_∞ and concentration C_∞ in the presence of ohmic heating and Dufour effect with a modified buoyancy model is incorporated into the flow formulation[13].

$$\frac{\partial u}{\partial x} + \frac{\partial v}{\partial y} = 0 \tag{1}$$

$$u\frac{\partial u}{\partial x} + v\frac{\partial u}{\partial y} = \frac{\mu_{nf}}{\rho_{nf}}\frac{\partial^2 u}{\partial y^2} - \frac{\sigma\beta_0^2}{\rho_{nf}}u - \frac{\mu_{nf}}{\rho_{nf}}\frac{1}{k}u + \frac{g\beta_{ep}}{\rho_{nf}}(T - T_\infty) + \frac{g\beta_c}{\rho_{nf}}(C - C_\infty) \tag{2}$$

$$u\frac{\partial T}{\partial x} + v\frac{\partial T}{\partial y} = \alpha_{nf}\frac{\partial^2 T}{\partial y^2} - \frac{1}{(\rho c_p)_{nf}}\frac{\partial q_r}{\partial y} + \frac{\mu_{nf}}{(\rho c_p)_{nf}}\left(\frac{\partial u}{\partial y}\right)^2 + \frac{D_m k_{nf}}{C_s C_p}\frac{\partial^2 C}{\partial y^2} + \frac{\sigma\beta_0^2}{(\rho c_p)_{nf}}u^2 \tag{3}$$

$$\rho_{nf}\left(u\frac{\partial C}{\partial x} + v\frac{\partial C}{\partial y}\right) = \frac{D_m k_t}{C_s C_p}\frac{\partial^2 C}{\partial y^2} + \frac{D_m k_{nf}}{\tau}\frac{\partial^2 T}{\partial y^2} - k_0(C - C_\infty) \tag{4}$$

where u and v are the velocity component in the x and y direction respectively. β_{ep} is the volumetric coefficient of thermal expansion of nanofluid, T is the temperature, C is the concentration of the nanofluid, C_∞ is the ambient concentration, q_r is the radiative heat flux, D_m is the mass diffusivity, k_f is the thermal diffusion ratio C_s is the concentration susceptivity, C_p is specific heat at constant pressure, τ is the thermophoretics, B_0 is the magnetic field, k is the permeability of the porous medium, k_0 is the chemical reaction and σ is the electrical conductivity. The dynamic viscosity of the nanofluid (μ_{nf}), effective density of the nanofluid (ρ_{nf}), thermal conductivity of the nanofluid (α_{nf}) and heat capacitance of the nanofluid $(\rho c_p)_{nf}$[19].

$$\mu_{nf} = \frac{\mu_f}{(1-\phi)^{2.5}}, \rho_{nf} = (1-\phi)\rho_f + \phi\rho_s, \alpha_{nf} = \frac{k_{nf}}{(\rho c_p)_{nf}}$$

$$(\rho c_p)_{nf} = (\rho c_p)_f \left((1-\phi) + \phi \frac{(\rho c_p)_s}{(\rho c_p)_f} \right)$$

The thermal conductivity of nanofluid of a spherical Nanoparticle is given as [26]:

$$k_{nf} = k_f \left[\frac{k_s + 2k_f - 2\emptyset(k_f - k_s)}{k_s + k_f - \emptyset(k_f - k_s)} \right] \tag{6}$$

where f and s are the subscript of the quantities in the base fluid and nanoparticles respectively. According to the Roseland diffusion approximation the radiative heat flux q_r is given by

$$q_r = -\frac{4\sigma^*}{3k^*}\frac{\partial T^4}{\partial y} \tag{7}$$

where σ^* and k^* are the Stefan-Boltzmann constant and the Rosseland mean absorption coefficient respectively. We assumed that the temperature difference within the flow are sufficiently small such that T^4 may be expressed as a linear function of temperature.

$$T^4 \approx 4T_\infty^3 T - 3T_\infty^4 \tag{8}$$

Substituting Equation (8) into Equation (7) and differentiate with respect to y, we have;

$$q_r = -\frac{4\sigma^*}{3k^*}\frac{\partial}{\partial y}(4T_\infty^3 T - 3T_\infty^4) = -\frac{4\sigma^*}{3k^*}4T_\infty^3\frac{\partial T}{\partial y} = -\frac{16\sigma^* T_\infty^3}{3k^*}\frac{\partial T}{\partial y}$$

$$\frac{\partial q_r}{\partial y} = -\frac{16\sigma^* T_\infty^3}{3k^*}\frac{\partial^2 T}{\partial y^2} \tag{9}$$

Substituting (9) into (3), we have

$$u\frac{\partial T}{\partial x} + v\frac{\partial T}{\partial y} = \frac{\alpha_{nf}}{(\rho c_p)_{nf}}\frac{\partial^2 T}{\partial y^2} - \frac{16\sigma^* T_\infty^3}{3k^*(\rho c_p)_{nf}}\frac{\partial^2 T}{\partial y^2} + \frac{\mu_{nf}}{(\rho c_p)_{nf}}\left(\frac{\partial u}{\partial y}\right)^2 + \frac{D_m k_{n_f}}{C_s C_p}\frac{\partial^2 C}{\partial y^2} + \frac{\sigma\beta_0^2}{(\rho c_p)_{nf}}u^2 \tag{10}$$

The appropriate boundary conditions for the problem are:

$$u = U_W = bx, v = 0, T = T_w = T_\infty + A\left(\frac{x}{l}\right)^2, C = C_w = C_\infty + B\left(\frac{x}{l}\right)^2 \ \ at\ y = 0$$
$$u \to 0, T \to T_\infty, C \to C_\infty \ \ as\ y \to \infty \tag{11}$$

Provided that *A*, *B and b* are constant, $b > 0$ A and B are the area of emitting body of the temperature and concentration equation respectively and l is the characteristics length.

III Method of Solution

We seek a similarity solution using the stream functions similar to Shankar and Eshetu[26], define as

$$\psi = (b\nu_f)^{1/2} x f(\eta), \eta = \left(\frac{b}{\nu_{nf}}\right)^{1/2} y \tag{12}$$

Then the longitudinal and axial component of the velocity, u and v are

$$u = \frac{\partial\psi}{\partial y} = \eta_y\psi_\eta = \left(\frac{b}{\nu_{nf}}\right)(b\nu_{nf})^{1/2} x f'(\eta) = bx f'(\eta),$$
$$v = -\frac{\partial\psi}{\partial x} = -(b\nu_{nf})^{1/2} f(\eta) \tag{13}$$

and the similarity variable for energy and species concentration are defined as:

$$g(\eta) = \frac{T - T_\infty}{T_w - T_\infty}, h(\eta) = \frac{C - C_\infty}{C_w - C_\infty} \tag{14}$$

Using equations (12), (13) and (14) in equations (1), (2), (4) and (10), we have

$$\frac{\partial u}{\partial x} + \frac{\partial v}{\partial y} = bf'(\eta) - \eta_y(b\nu_f)^{1/2} f(\eta) = bf'(\eta) - bf'(\eta) = 0$$

Equation (1) is identically satisfied!

We perform similar procedures on momentum, energy and chemical species concentration gives,

$$f'''(\eta) + \left[(f(\eta)f''(\eta) - f'(\eta)^2)\left((1-\phi) + \phi S_G\right)\right]\sqrt{(1-\phi)^5} \\ [+Grtg(\eta) + Grch(\eta) - Mf'(\eta)]\sqrt{(1-\phi)^5} - k_1 f'(\eta) = 0 \quad (15)$$

$$\left(1+\frac{4R}{3}\right)g''(\eta) + PrEc(f''(\eta)^2(1-\phi)^{2.5} + Mf'(\eta)^2) \\ -Pr\left((1-\phi) + \phi\frac{(\rho c_p)_s}{(\rho c_p)_f}\right)\left(2f'(\eta)g(\eta) - f(\eta)g'(\eta) - Duh''(\eta)\right) \quad (16)$$

$$h''(\eta) + Srg''(\eta) - Sc\gamma h(\eta) - Sc\left((1-\phi) + \phi S_G\right)\left(2f'(\eta)h(\eta) - f(\eta)h'(\eta)\right) \quad (17)$$

With the associated boundary conditions as;

$$f'(\eta) = 1, f(\eta) = 0, g(\eta) = 1, h(\eta) = 1 \ \ at\ \eta = 0 \\ f'(\eta) \to 0, g(\eta) \to 0, h(\eta) \to 0 \qquad as\ \eta \to \infty \quad (18)$$

Where

$$\left.\begin{aligned} &\frac{(\mu c_p)_f}{k_f} = Pr, \frac{D_m k_f}{C_s C_p}\frac{(C_w - C_\infty)}{(T_w - T_\infty)}\frac{1}{\nu_f} = Du, \frac{1}{k_t}\frac{u_w^2}{(T_w - T_\infty)x^2 c_{p_f}} = Ec, \frac{\nu_f}{bk} = k_1, \frac{\rho_s}{\rho_f} = S_G, \\ &\frac{g\beta_{ep}}{bx\rho_f}(T_w - T_\infty) = Grt, \frac{g\beta_c}{bx\rho_n}(C_w - C_\infty) = Grc, \qquad Re_x = \frac{xu_w}{\upsilon_f}, \frac{4\sigma^* T_\infty^3}{k^* k_f k_t} = R_d, \\ &\frac{D_m}{\mu_f} = \frac{1}{Sc}, \frac{k_0}{\rho_f b} = \gamma, \frac{D_1}{D_m}\frac{(T_w - T_\infty)}{(C_w - C_\infty)} = Sr, A = (T_w - T_\infty)l, B = (C_w - C_\infty)l \end{aligned}\right\} \quad (19)$$

Rate of Flow at the wall: Engineering parameters of curiosity in the flow are skin friction coefficient C_f and Nusselt number Nu_x and local Sherwood number Sh_x defined respectively as;

$$C_f = \frac{2\tau_w}{\rho_f u_w^2}, \tau_w = -\mu_{nf}\left(\frac{\partial u}{\partial y}\right)_{y=0}$$

$$Nu_x = \frac{xq_w}{k_f(T_w - T_\infty)}, q_w = -\left(k_{nf} + \frac{16\sigma^* T_\infty^3}{3k^*}\right)\left(\frac{\partial T}{\partial y}\right)_{y=0}$$

$$Sh_x = \frac{xJ_w}{D(C_w - C_\infty)}, J_w = -D\left(\frac{\partial C}{\partial y}\right)_{y=0}$$

Using similarity transformation, we have
This implies

$$C_f = -\frac{2f''(0)}{(1-\phi)^{2.5}} \quad (20)$$

$$Nu_x = -k_T\sqrt{Re_x}\left(1+\frac{4R_d}{3}\right)g'(0) \quad (21)$$

$$Sh_x = -\sqrt{Re_x}h'(0) \quad (22)$$

The above equations (20) – (22) are that the *skin friction coefficient (surface drag)*, rate of heat transfer at the wall and rate of mass transfer at the wall respectively.

Table 1: Thermo-physical properties of water and copper Motsumi

Physical properties	Copper(Cu)	Base fluid(Water)
$C_p(JKg^{-1}k)$	385	4179
$\rho(kg/m^3)$	8933	997.1
$\kappa(W/mK)$	400	0.613
$\rho C_p(Jkg^{-1}kkg/m^3)$	3439205	4,166,880.9

Equation (15) – (17) subject to boundary conditions (18) are solved using midpoint methods known as midrich method with Richardson extrapolation enhancement or deferred correction enhancement, the midpoint sub methods are capable of handling harmless end-point singularities that other submethods cannot. For the enhancement schemes, Richardson extrapolation is generally faster, but deferred corrections uses less memory on difficult problems. The computations are implemented using Maple 2021. The result of the computation are presented and discussed below.

IV. Results and Discussion

The effects of various parameters such as the volume fraction (ϕ), thermal radiation parameter (R), Buoyancy coefficient (Grt), Buoyancy coefficient ratio (Grc)scaled chemical reaction parameter (γ), Magnetic parameter (M), porous medium parameter (k_1), Eckert number (Ec), Dufour number (Du), prandtl number (Pr), Schmidt number (Sc), Soret number (Sr) and the nanofluid density ratio of particles and base fluid parameter (S_G) on the Velocity $f(\eta)$, Temperature $g(\eta)$ and Concentration $h(\eta)$ as well as rate of heat and mass transfer at the wall are presented and discussed in the figures below. Figure 2 shows the effect of thermal radiation parameter on the velocity profile. It is observed that an increase in the thermal radiation parameter increases both velocity and momentum boundary layer. Figure 3 depicts the effect of volume fraction on the velocity profile. It could be observed that increase in volume fraction of nanoparticles enhances the bulk momentum of the flow. In fact introduction of nanoparticles in the flow properties could be used to minimize the effect of Lorentz force. The velocity of the fluid decreases as the volume fraction increases. Figure 4 shows the scaled chemical reaction effect on the bulk velocity of the flow. It could deduced from the figure that the increase in the reaction parameter leads to the decrease in the velocity of the fluid. Figure 5 - 6 shows the effect of Buoyancy coefficient on the velocity profile respectively. It is observed from both figure that the velocity increases as the Buoyancy parameter increases. Figure 7 shows the effect of the magnetic parameter on the velocity profile. The velocity tends to decreased when there is an increase in the magnetic parameter. This is typical of Lorentz force which usually opposes velocity, however, the effect could be minimized by the introduction of nanoparticles to enhance the flow. Figure 8 indicates the effect of density ratio of nanoparticle and based fluid. The increase in leads to a decreasing effect in the fluid velocity. Figure 9 depicts the effect of the porous medium parameter on the fluid velocity. It is observed that the increase in the porous medium parameter also brings about the decreasing effect of the fluid velocity. Figure 10 shows the effect of Eckert number on the velocity profile. It is noticed that the increase in the Eckert number brings about the increase in the velocity of the fluid. Figure 11 shows the effect of Dufour number on the velocity profile. The increasing effect of the fluid velocity is as a result of the increase in the Dufour number. Figure 12 indicates the effect of Prandtl number on velocity profile. It is noticed from the figure that the increase in the Prandtl number, brings about the decrease in the fluid velocity. This is true because higher values of Prandtl number indicate lover conductivity and hence viscousity dominates. Figure 13 shows the effect of the thermal radiation parameter on the temperature profile. From the figure, it is observed from the figure that the temperature increases as a result of increasing the thermal radiation parameter. Figure 14 depicts the effect of volume fraction on temperature. It is observed that temperature increases as there is an increase in the volume fraction of the nanofluid. Figure 15 shows the effect of Buoyancy coefficient factor on temperature profile. A decreasing effect is observed in the temperature as a result of the increase in the Buoyancy coefficient factor. Figure 16 shows the effect of Magnetic parameter on temperature profile. From the figure it is observed that temperature increases as a result of an increase in the magnetic parameter. Figure 17 indicates the effect of porous medium parameter on temperature profile. The increase in the porosity brings about the increase in the temperature of the fluid as shown in the figure. It is observed from Figures 18 and 19 that an increase in the Eckert and Dufour number respectively, result in increase in thermal boundary layer. At higher values of both Ecket and Dufour number, a peak was observed on the profile. That is an indication that maximum temperature occurs in the body of the fluid contrary to general believe that the maximum temperature is at the surface. Figure 20 Analyses the effect of prandtl number on temperature profile. It is observed that with the increase in the prandtl number, the temperature of the fluid decreases. Figure 21 depicts the effect of scaled chemical reaction on concentration profile. A decreasing effect is shown in the concentration of the fluid with an increase in the scaled chemical reaction parameter as indicated in the figure. Figure 22 shows the effect of thermal Buoyancy coefficient factor on concentration profile. A decreasing effect is observed in the concentration as a result of the increase in the Buoyancy coefficient factor. Figure 23 shows the effect of Magnetic parameter on concentration profile. From the figure it is observed that concentration increases as a result of an increase in the magnetic parameter. Figure 24 indicates the effect of nanofluid density ratio of particles and base fluid parameter on concentration profile. It is observed from the figure that when there is an increase in the nanofluid density ratio of particles and base fluid parameter, the concentration of the fluid decreases. Figure 25 depicts the effect of porous medium parameter on concentration profile. There is an increase in concentration of the fluid with an increase in the porous medium parameter as indicated in the figure. Figure 26 shows the effect of Soret number on concentration profile. From the figure, an increasing effect is noticed in the fluid velocity as the Soret number is been increased. Figure 27 depicts the effect of Schmidt number on concentration profile. It is observed that a decreasing effect of concentration of fluid occurs as a result of increase in the Schmidt number parameter.

Table 1: Standard values for the governing parameters

Parameters	R	Grc	Grt	M	ϕ	S_G	γ	k_1	Ec	Sc	Pr	Du	Sr
Value	2	5	10	0.5	1	3.4	0.08	1	1	0.6	0.71	0.5	0.2

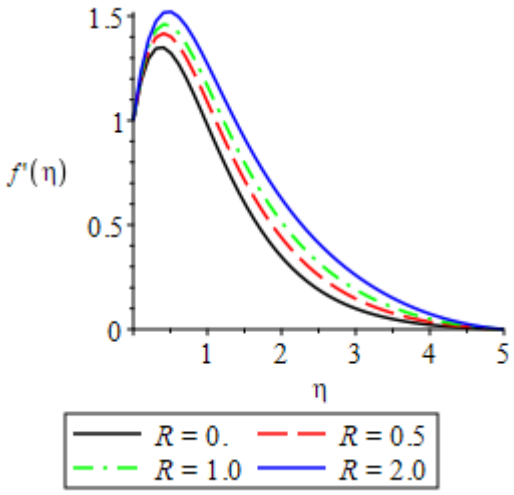

Figure 2: Effect of Thermal Radiation Parameter (R) on the velocity profile.

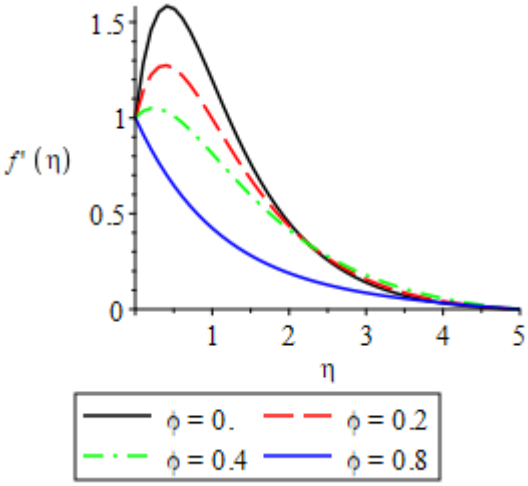

Figure 3: Effect of volume fraction $(\emptyset)$ on the velocity profile.

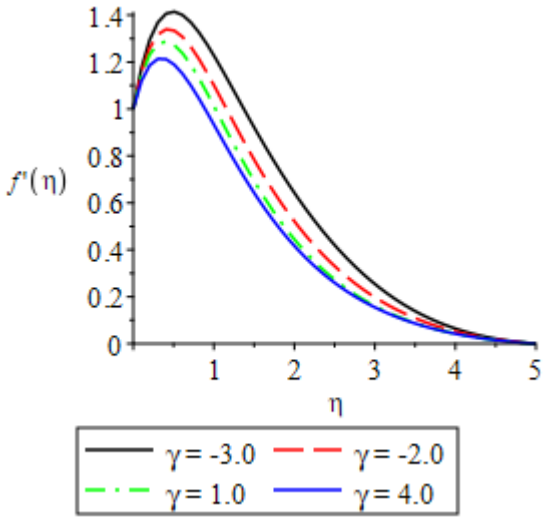

Figure 4: Effect of scaled chemical reaction (γ) on the velocity profile

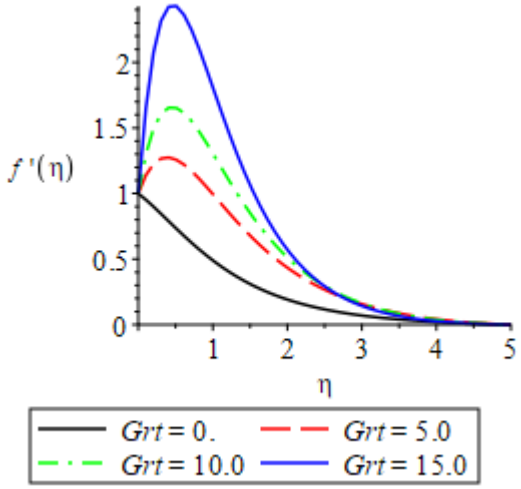

Figure 5: Effect of Buoyancy coefficient factor (Grt) on the velocity profile.

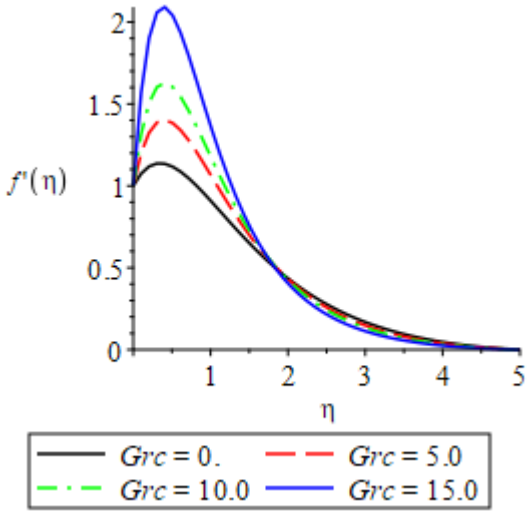

Figure 6: Effect of Buoyancy coefficient (Grc) on velocity profile

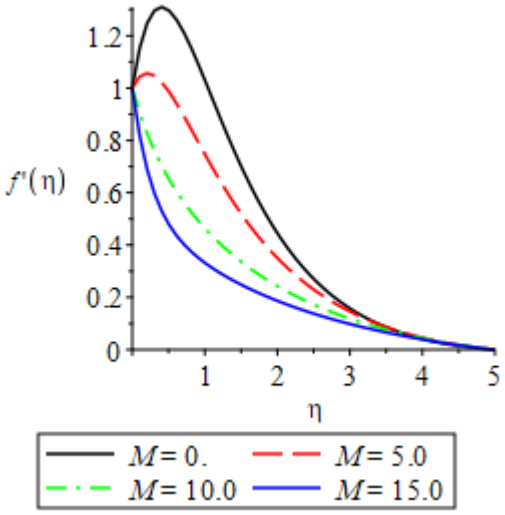

Figure 7: Effect of Magnetic parameter (M) on the velocity profile

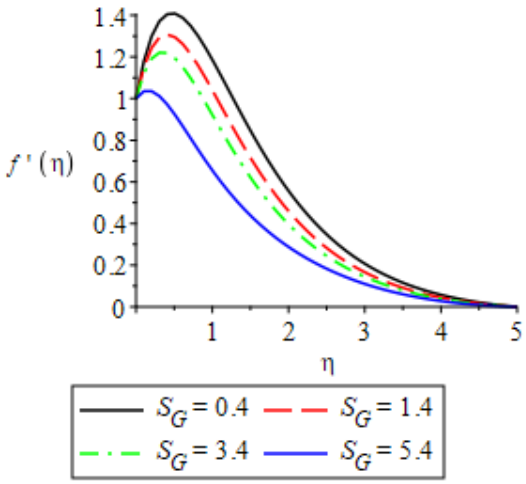

Figure 8: Effect of the ratio of nanoparticle and based fluid (S_G) on velocity profile

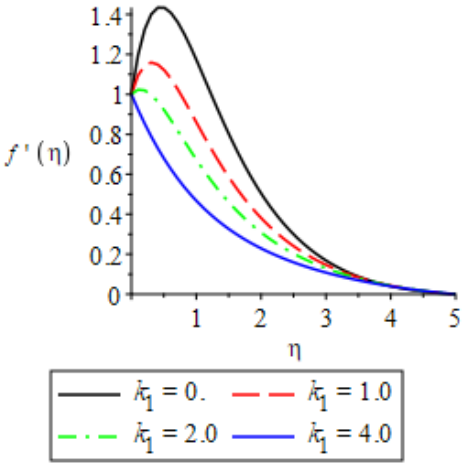

Figure 9: Effect of the porous medium parameter (k_1) on velocity profile

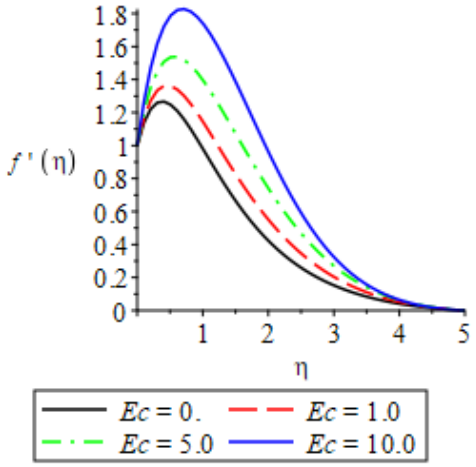

Figure 10: Effect of Eckert number (Ec) on velocity profile

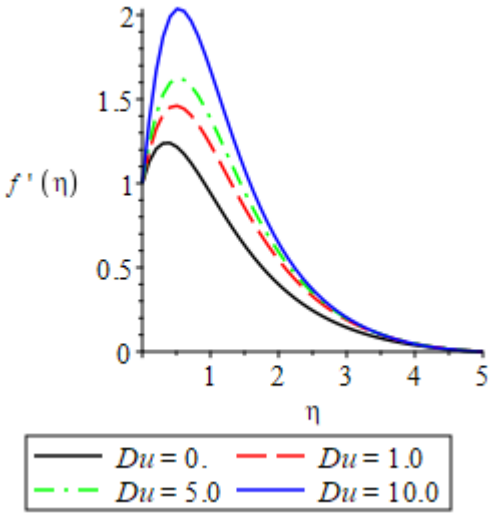

Figure 11: Effect of Dufour number (Du) on velocity profile

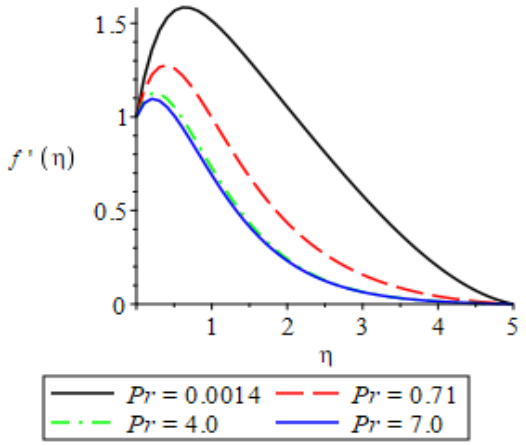

Figure 12: Effect of Prandtl number (Sr) on velocity profile

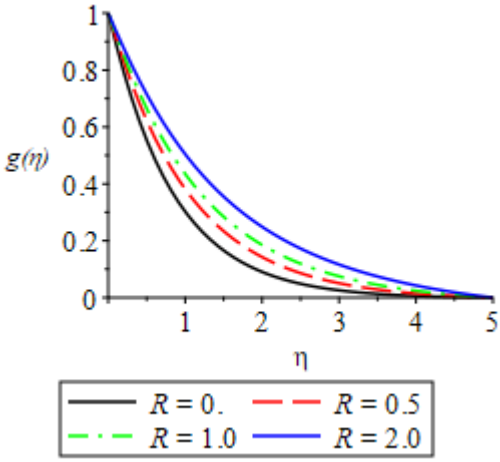

Figure 13: Effect of Thermal Radiation Parameter (R) on Temperature profile

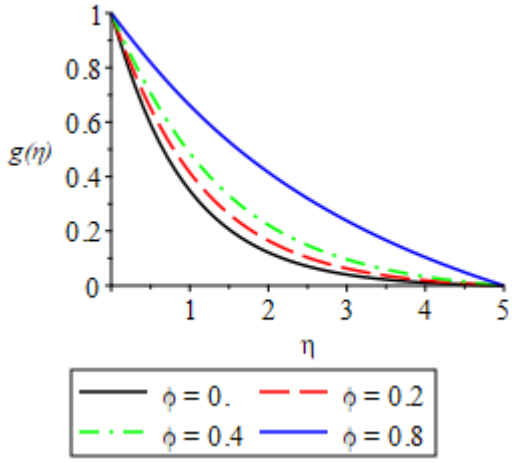

Figure 14: Effect of Volume fraction $(\emptyset)$ on Temperature profile.

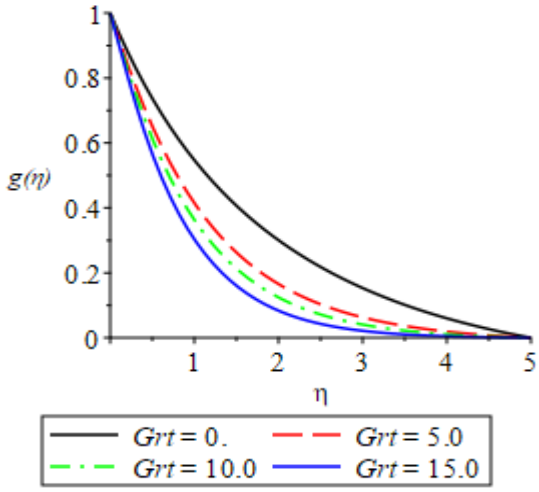

Figure 15: Effect of Buoyancy Coefficient factor (Grt) on Temperature profile.

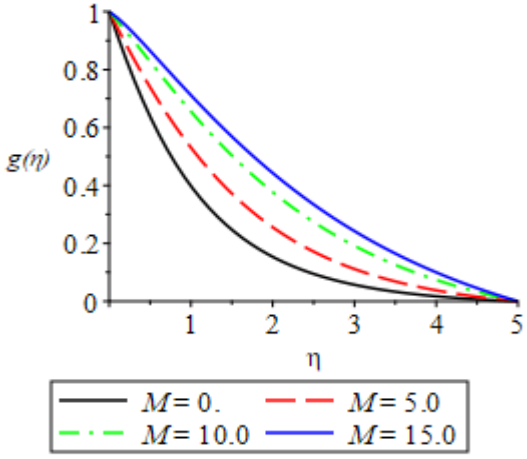

Figure 16: Effect of Magnetic parameter (M) on Temperature profile.

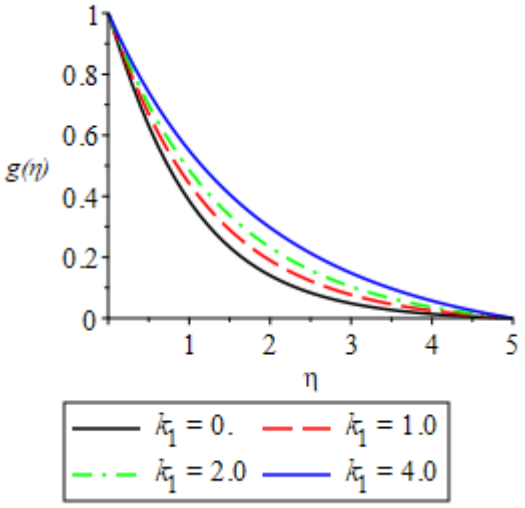

Figure 17: Effect of Porous medium parameter (k_1) on Temperature profile.

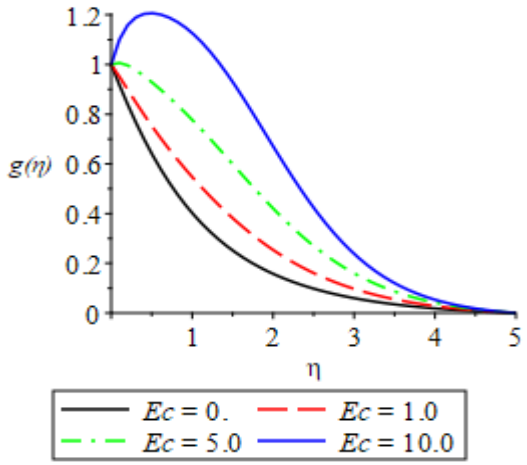

Figure 18: Effect of Eckert number (Ec) on the Temperature profile.

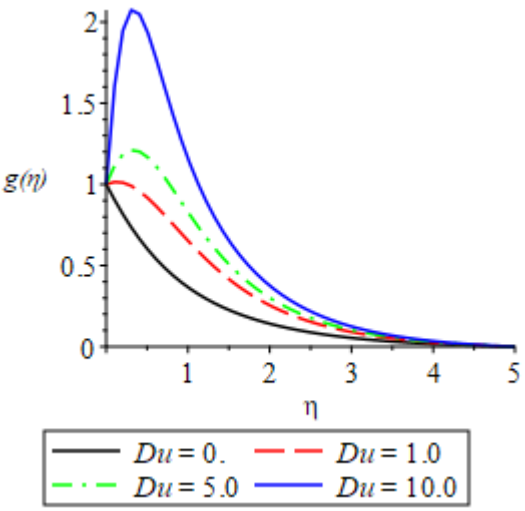

Figure 19: Effect of Dufour number (Du) on Temperature profile.

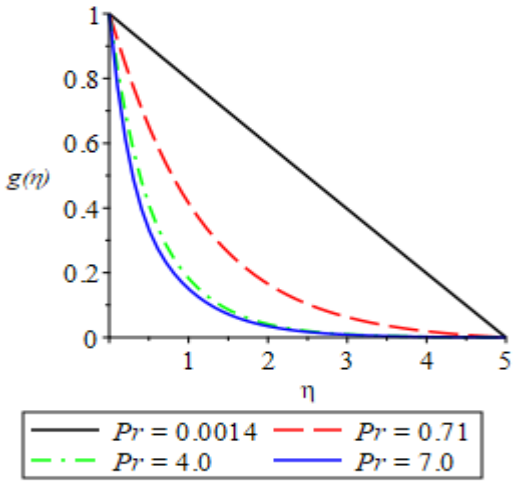

Figure 20: Effect of Prandtl number (Pr) on Temperature profile.

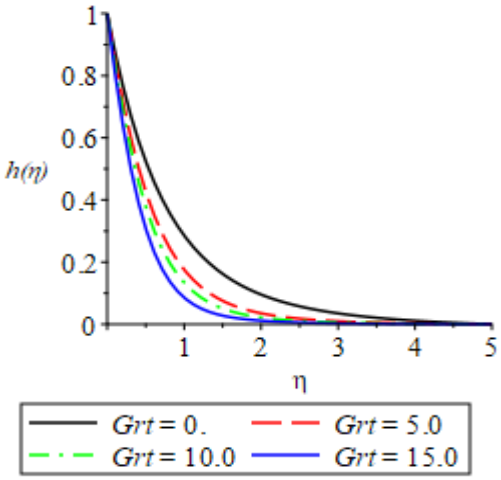

Figure 22: Effect of Buoyancy Coefficient (Grt) on Concentration profile.

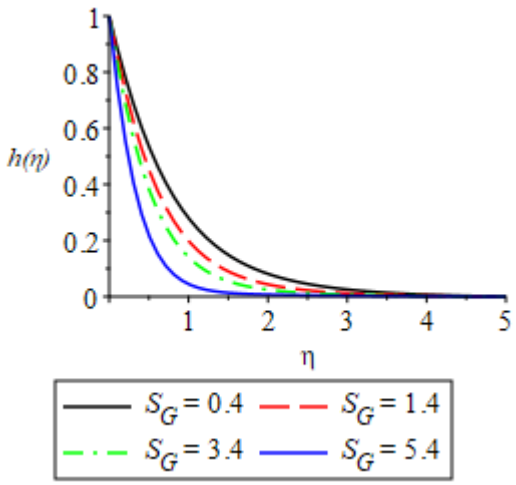

Figure 24: Effect of the density ratio of nanoparticle and based fluid (S_G) on concenntration profile.

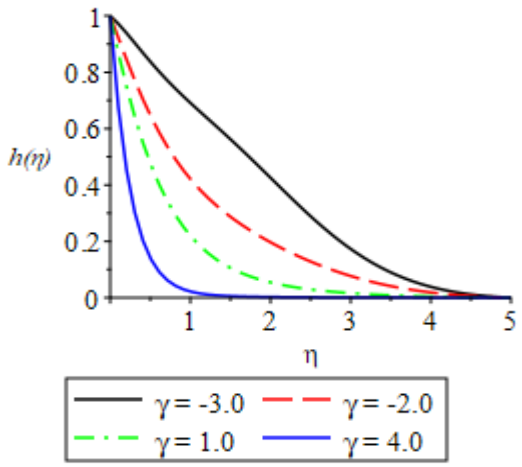

Figure 21: Effect of Scaled Chemical Reaction (γ) on Concentration profile.

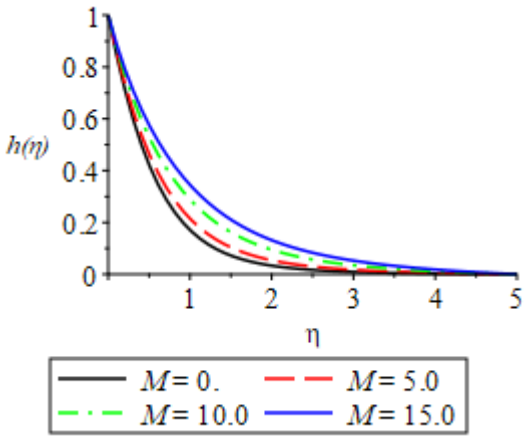

Figure 23: Effect of Magnetic parameter (M) on Concentration profile.

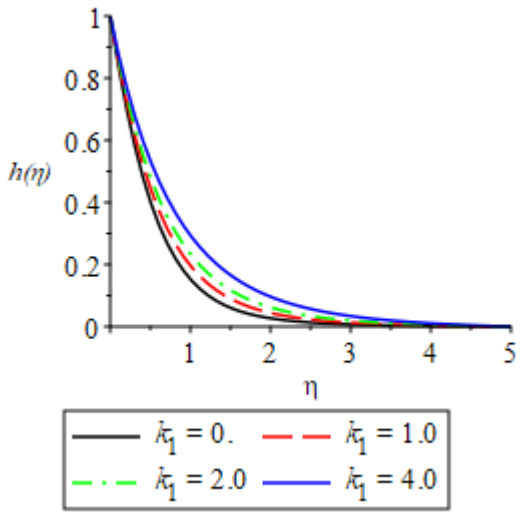

Figure 25: Effect of Porous medium parameter (k_1) on Concentration Profile.

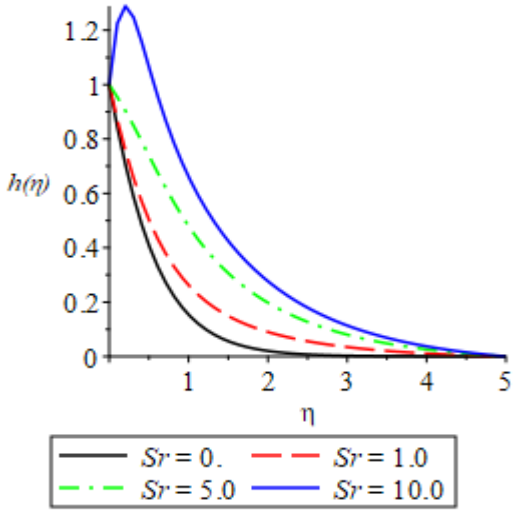

Figure 26: Effect of Soret number (Sr) on Concentration profile.

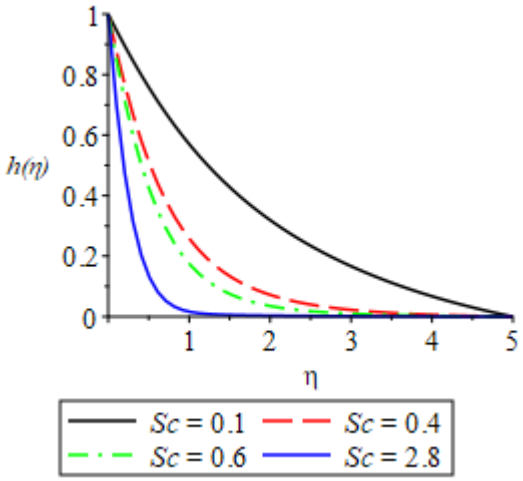

Figure 27: Effect of Schmidt number on Concentration Profile.

V. Conclusion

The study on Buoyancy effect on Magnetohydrodynamics (MHD) Nanofluid flow over a porous medium in the presence of Dufour and Ohmic Heating has been investigated. The transformed governing equations with the boundary conditions are solved numerically using midpoint method with Richardson extrapolation enhancement and deferred correction enhancement, the midpoint submethods are capable of handling harmless end-point singularities that other submethods cannot. For the enhancement schemes, Richardson extrapolation is generally faster. The computations are implemented using Maple 2021. The result of the computation are presented and discussed below. Some of the interesting observations of the study are as follow:

i. There is a decrease in the velocity of the fluid, as the nanofluid volume fraction and the scaled chemical parameter increases.
ii. The increase in the thermal radiation and the Eckert number increases the velocity and temperature of the nanofluid.
iii. The velocity of fluid increases as the Buoyancy coefficient factor and the Buoyancy coefficient ratio is increases.
iv. The velocity of the cu-water nanofluid decreased, while temperature and concentration of the nanofluid increases when there is an increase in the Magnetic parameter.
v. Chemical reaction parameter and Schmidt number reduce the concentration profile while the Soret number enhances the concentration profile.
vi. The presence of nanoparticle volume fraction, thermal radiation and porous media in the flow field is to reduce the rate of thermal boundary layer thickness of nanofluids.
vii. The increase in the porous medium parameter decreases the fluid velocity and increase temperature and concentration of the cu-water nanofluid.
viii. The presence of Prandtl number and Schmidt number reduces the flow of the nanofluid.
ix. The velocity and temperature of the nanofluid increases when the Dufour number undergoes an increasing effect.

Table 2 shows the effects of the various parameters on the skin friction $f''(0)$, temperature gradient $g'(0)$ and concentration gradient $\mathrm{h}'(0)$. It is observed from the table that the increase in the Thermal radiation parameter brings about the increase in the skin friction, rate of heat transfer at the wall and a decrease in the concentration gradient. The increase in the nanofuid volume fraction results in the decrease in skin friction, increase in the rate of heat transfer at the wall and decrease in the concentration gradient. Also, there is a decrease in the skin friction an increase in the rate of heat transfer at the wall and a decrease in the concentration gradient when the scaled chemical reaction parameter has an increasing effect and when there is increase in the

Buoyancy coefficient factor and the Buoyancy coefficient ratio, the skin friction increases, the rate of heat and mass transfer at the wall decreases respectively. It is also observed that an increase in the Magnetic parameter brings about the decrease in the skin friction increase in the rate of heat transfer at the wall and concentration gradient and the increase in the nanofluid density ratio of particles and base fluid parameter results in the increase in the temperature gradient and decrease in the skin friction and concentration gradient

Table 3 shows the effect of porous medium parameter, Eckert number, Dufour number (Du), Soret number (Sr), Prandtl number (Pr) and Schmidt number (Sc) on skin friction, temperature gradient and concentration gradient From the table, the increase in the porous medium parameter decreases the skin friction and enhances the rate of heat and mass transfer at wall. An increase in the skin friction, decrease in rate of heat and mass transfer at wall is observed when there is an increase in the Eckert number, while increase in the Dufour number enhances the skin friction and rate of heat transfer at wall and reduces the rate of mass transfer at wall. Increase in the Soret number is observed to enhances the skin friction and rate of mass transfer at the wall while, a decrease in the energy transfer at the wall is observed. The skin friction and the heat transfer at the wall decreases, while the mass transfer at the wall is enhanced as a result of the increase in the Prandtl number. Also, when there is an increase in the Schmidt number the skin friction and rate of mass transfer at the wall decreases, while rate heat transfer at the wall is enhanced.

Table 2: Effect of $R, \phi, \gamma, Grt, Grc, M$ and S_G

R	ϕ	γ	Grt	Grc	M	S_G	$f''(0)$	$\theta'(0)$	$\phi'(0)$
0	1.0	0.08	10.0	5.0	0.5	3.4	2.25859	-1.10069	-1.42527
0.5							2.44407	-0.88041	-1.48702
1.0							2.56163	-0.76175	-1.52152
2.0							2.70973	-0.62847	-1.56073
	0						3.35664	-0.95012	-1.37763
	0.2						1.67655	-0.80506	-1.57797
	0.4						0.46938	-0.65344	-1.71513
	0.8						-0.87639	-0.37634	-1.89031
		-3.0					2.03207	-1.04299	-0.24384
		-2.0					1.85596	-0.95156	-0.76761
		1					1.71401	-0.84498	-1.35547
		4					1.4677	-0.39803	-3.83646
			0				-0.43338	-0.61572	-1.30999
			5				1.67655	-0.80506	-1.57797
			10				3.51351	-0.87565	-1.73609
			15				7.64738	-0.90024	-2.01261
				0			0.90353	-0.77438	-1.51404
				5			2.41186	-0.82778	-1.63354
				10			3.79961	-0.8567	-1.72833
				15			6.95348	-0.87044	-1.91278
					0		1.81705	-0.8394	-1.59071
					5		0.60936	-0.57312	-1.47487
					10		-1.0043	-0.31016	-1.30537
					15		-2.12193	-0.1772	-1.18842
						0.4	2.08476	-0.91483	-1.17235
						1.4	1.78204	-0.83417	-1.47194
						3.4	1.48985	-0.75261	-1.76732
						5.4	0.55216	-0.47887	-2.74691

Table 3: Effect of k_1, Ec, Du, Sr, Pr and Sc

K_1	Ec	Du	Sr	Pr	Sc	$f''(0)$	$\theta'(0)$	$\phi'(0)$
0	3	5	5	0.71	0.6	2.26863	-0.84598	-1.64683
1						1.18264	-0.76708	-1.51877
2						0.38784	-0.70139	-1.42136
4						-0.77189	-0.60338	-1.27892
	0					1.65438	-0.83704	-1.56964
	1					1.91198	-0.45715	-1.66452
	2					2.31432	0.18074	-1.80772
	3					2.91385	1.2655	-2.02304
		0				1.57709	-0.9768	-1.53651
		3				2.1935	0.23475	-1.80238

		5				2.64209	1.36623	-2.02296
		10				4.06014	7.26057	-3.10572
			0			1.66205	-0.79498	-1.63171
			1			1.73726	-0.84894	-1.33874
			3			1.91514	-1.00778	-0.43702
			5			2.19198	-1.6407	3.11163
				0.001		2.33669	-0.20308	-1.74647
				0.71		1.67655	-0.80506	-1.57797
				4		1.16815	-1.76785	-1.33714
				7		1.0117	-2.43943	-1.19462
					0	2.17357	-1.08158	-0.02369
					0.4	1.74072	-0.86156	-1.26251
					0.6	1.67655	-0.80506	-1.57797
					2.8	1.47373	-0.48788	-3.34951

References

[1] Yahaya, S. D. and Simon, K. D., (2015), "Effect of Buoyancy and Thermal Radiation on MHD flow over a Stretching Porous Sheet using Homotopy Analysis Method".

[2] Subhas, M. A., Klkarni, A. K. and Ravikumara, R., (2011), "MHD flow and heat transfer with effects of buoyancy, viscosity and Joules dissipation over a nonlinear vertical stretching porous sheet with partial slip"., vol.3, No. 3, Doi:10.4236/eng.2011.33033

[3] Lakshmi, G. D., Niranja, H. and Sivasankara, S. (2021), "Effects of chemical reaction, radiation and activation energy on MHD buoyancy induced nanofluid flow past a vertical surface", *Transsaction B: Mechanical engineering, scientific Iranica B* (2022) 29(1), 90-100, DOI: 10.24200sci.56835.4934

[4] Animasaun I. L. and Sandeep, N., (2016) "Buoyancy induced model for the flow of 36 nm alumina-water nanofluid along upper horizontal surface of a paraboloid of revolution with variable thermal conductivity and viscosity" *Power Technology* **301**, 858 - 867. doi: /10.1016/j.powtec.2016.07.023

[5] Nguyen, C. T., (2012), "Fundamentals of Mass Transport in microscale,"., second edition, http://doi.org/1016/B978 - 1 - 4377-3520-8.00002 – 4.

[6] Nguyen CT, Desgranges F, Roy G, Galanis N, Mare T, Boucher S and Angue Minsta H, (2007), "Temperature and particle-size dependent viscosity data for water based nanofluids – hystresis phenomenon". *Int. J. Heat Fluid Flow* 28, 1492–1506 (2007).

[7] Angue M, Roy HG, Nguyen CT and Doucet D (2009) "New temperature and conductivity data for water-based nanofluids". *Int. J. Therm. Sci. 48* (2), 363–371,

[8] Abu-Nada, E. (2009) "Effects of variable viscosity and thermal conductivity of Al_2O_3water nanofluid" *Int. J. Heat Fluid Flow* (2009), doi: 10.1016/j.ijheatfluidflow.2009.02.003.

[9] Liu, M., Lin, M. C. and Wang, C. (2011) "Enhancements of thermal conductivities with Cu, CuO, and carbon nanotube nanofluids and application of MWNT/water nanofluid on a water chiller system." *Nanoscale Research Letter* 6, 297. doi:10.1186/1556-276X-6-297.

[10] Amireh, N., Hamdolah, M. and Morteza, B., (2019), "Effect of radiation and Magnetohydrodynamics (MHD) on heat Transfer of nanofluid flow over a plate"., SN Applied sciences (2019) |:1581|https://doi.org/10.1007|s42452-019-1634-6

[11] Musa, A. M., Verdiana, G. M., Eunice, W. M. and Makungu, N. J. (2019), "Unsteady MHD flow nanofluid with variable properties over a stretching sheet in the presence thermal radiation and chemical reaction", international journal of mathematics and mathematical science.

[12] Haile, E., & Shankar, B. (2014). Heat and mass transfer through a porous media of MHD flow of nanofluids with thermal radiation, viscous dissipation and chemical reaction effects. *American Chemical Science Journal*, *4*(6), 828-846.

[13] Makinde, O. D. and Animasaun, I. L. (2016),"Bioconvection in MHD nanofluid flow with nonlinear thermal radiation and quartic autocatalysis chemical reaction past an upper surface of a paraboloid of revolution," *International Journal of Thermal Sciences* **109**, 159 - 171.

[14] Durga, P. P. and Varma, S. V. K. (2018), "Heat and Mass Transfer Analysis for the MHD flow of nanofluid with radiation absorption", *Ain shams Engineering journal*, vol.9: pages 801 – 813. https://doi.org/10.1016/j.asej.2016.04.016

[15] Hunegnaw, D. and Nailoti, K. (2014), "MHD effect on heat transfer over stretching sheet embendded in porous medium with variable viscosity, viscous dissipation and heat source/sink", *Ain shams Engineering journal*, vol.9: pages 801 – 813. https://doi.org/10.1016/j.asej.2014.03.008

[16] Salengke, S. (2000). Electrothermal Effects of Ohmic Heating on Biomaterials Temperature Monitoring, Heating of Solid-Liquid Mixtures and Pretreatment Effects on Drying Rate and Oil Uptake. *Unpublished Ph.D. Dissertation. The Ohio State University, United States of America.*

[17] Evaline Chepkemoi, Wilys O. Mukuna (2021): Hydromagnetic Free Convection Unsteady Turbulent Fluid Flow Over A Vertical Infinite Heat Absorbing Plate. *IOSR Journal of Mathematics (IOSR-JM), Volume 17, Issue 3 Ser. I (May – June 2021), PP 42-48*, DOI: 10.9790/5728-1703014248 www.iosrjournals.org.

[18] Akindele Akintayo Oladimeji, Ajala Olusegun Adebayo, Adegbite Peter, Ogunsola Amos Wale: Convective Flow of Nanofluids Using Blasius-Rayleigh-Stoke Variable with Slip Effect. *IOSR Journal of Mathematics (IOSR-JM), Volume 17, Issue 3 Ser. I (May – June 2021), PP 01-08*. DOI: 10.9790/5728-1703010108 www.iosrjournals

[19] P.RameshBabu, Khaja Hassan, R.VijayaKumar: Radiation Effect on Unsteady Mixed Convective MHD Flow of Heat and Mass Transfer over An Accelerated Infinite Vertical Porous Plate With Suction And Chemical Reaction. *IOSR Journal of Mathematics (IOSR-JM), Volume 18, Issue 2 Ser. I (Mar. – Apr. 2022), PP 32-41. www.iosrjournals.org*. DOI: 10.9790/5728-1802013241 www.iosrjournals.org.

[20] A. M. Okedoye and P. O. Ogunniyi (2019): MHD Boundary Layer Flow Past a Moving Plate with Mass Transfer and Binary Chemical Reaction. Journal of the Nigerian Mathematical Society, Vol. 38, Issue 1, pp. 89-121.

[21] A. M. Okedoye and S. O. Salawu (2019): Unsteady oscillatory MHD boundary layer flow past a moving plate with mass transfer and binary chemical reaction. SN Applied Sciences (2019) 1:1586 https://doi.org/10.1007/s42452-019-1463-7.

[22] Akindele M. Okedoye and Sulyman O. Salawu (2019): Effect of Nonlinear Radiative Heat and Mass Transfer on MHD Flow over a Stretching Surface with Variable Conductivity and Viscosity. Journal of the Serbian Society for Computational Mechanics / Vol. 13 / No. 2, 2019 / pp 86-103 (10.24874/jsscm.2019.13.02.07).
[23] A.M. Okedoye and S.O. Salawu (2020): transient heat and mass transfer of hydromagnetic effects on the flow past a porous medium with movable vertical permeablesheet. Int. J. of Applied Mechanics and Engineering, 2020, vol.25, No.4, pp.175-190. DOI: 10.2478/ijame-2020-0057.
[24] Akindele M. Okedoye, Sulyman O. Salawu, and Raphael E. Asibor (2021): a convective MHD double diffusive flow of a binary mixture through an isothermal and porous moving plate with activation energy. Computational Thermal Sciences, 13(5):45–60 (2021).
[25] Sastry, S. k and Palaniappan, S, (1992). Ohmic Heating of Liquid-particle Mixtures, *Journal of Food Technology*, **46**: 64–70.
[26] Shankar, B. and Eshetu, H. (2014). Heat and Mass Transfer through a Porous Media of MHD Flow of Nanofluid with Thermal Radiation, Viscous Dissipation and Chemical Reaction Effect. *American Chemical Science Journal*, 4(6): 828-846.

A. M. Okedoye, et. al. "Buoyancy Effect on MHD Nanofluid flow over a Porous Medium In the presence of Dufour and Ohmic Heating." *IOSR Journal of Mathematics (IOSR-JM)*, 18(2), (2022): pp. 26-39.